

Transient receptor potential canonical type 3 channels facilitate endothelium-derived hyperpolarization-mediated resistance artery vasodilator activity

Supplementary Data

Supplementary Methods, Results, Discussion and Tables

2. Methods

2.1 Animals and tissue

Adult male Sprague Dawley rats were anaesthetised with sodium pentathol (100 mg/kg; ip), and ~300 μm diameter 1st-3rd order mesenteric arteries dissected in Krebs' solution containing (in mM): 112 NaCl, 25 NaHCO₃, 4.7 KCl, 1.2 MgSO₄.7H₂O, 0.7 KH₂PO₄, 10 HEPES, 11.6 glucose, 2.5 CaCl₂.2H₂O; pH 7.3. Male 8-10 week old TRPC3 KO mice¹ generated on a 129SvEv/C57BL/6J mixed background and age-matched littermate WT controls were anaesthetized with isofluorane and the aorta dissected in Hank's balanced salt solution for imaging studies. Rat liver, and mouse liver, aorta and mesenteric arteries were also dissected from anaesthetized (sodium pentathol; 100 mg/kg; ip) animals for reagent characterization studies. Respiration rate and tactile responses were monitored to indicate adequacy of anaesthesia.

KO and WT mice were genotyped via PCR amplification of the genomic TRPC3 DNA. The genotyping confirmed the omission of exon 7 of the TRPC3 gene in the KO mice as reported by Hartmann et al.¹

All procedures conform with the Guide for the Care and Use of Laboratory Animals published by the US National Institutes of Health (NIH Publication No. 85-23, revised 1996),

and were approved by the Animal Experimental Ethics Committees of the University of New South Wales (09/43B) and Monash University (SOBSA/P/2007/100), and the Animal Protocol Review Committee, Baylor College of Medicine (AN-4366).

2.2 Reagent characterization

TRPC3 antibody specificity was determined by immunohistochemistry using stably transfected HEK-293 cells expressing mouse TRPC3 (Supplementary material online, *Figure S1A-C*), and by confocal immunohistochemistry (Supplementary material online, *Figures S1D-I, S2A*) and Western blotting using extracts of tissues from rat (Supplementary material online, *Figure S3*). Primary antibody and primer characteristics are detailed in Supplementary material online, *Tables S1* and *S2*.

The specificity of the putative TRPC3 blocker Pyr3 (ethyl-1-(4-(2,3,3-trichloroacrylamide)phenyl)-5-(trifluoromethyl)-1H-pyrazole-4-carboxylate)² was validated by pressure myography in mesenteric artery from KO and WT mice, patch clamp using freshly isolated mouse mesenteric artery endothelial cells (Supplementary material online, *Figure S5*) and transfected HEK cells expressing TRPC3 (Supplementary material online, *Figure S4*) and by calcium imaging using aortic endothelial cells obtained from KO and WT mice (Supplementary material online, *Figure S2B*).

2.3 Western blotting

The specificity of TRPC3 antibody and characteristics of TRPC3 channels in adult male Sprague Dawley rat mesenteric artery were determined using Western blotting. Rat mesenteric arteries and liver, and mouse liver were rapidly frozen, and stored in liquid nitrogen. Tissues were ground using a mortar and pestle, resuspended in phosphate buffered saline (PBS), pH 7.4, containing

protease inhibitor cocktail (Roche Diagnostics, Castle Hill, Australia) and centrifuged (3000 x g, 4°C; 5 minutes). The supernatant was removed and placed on ice, and the pellet snap frozen and reprocessed as above. Supernatants were then pooled and centrifuged (20,000 x g, 4°C; 1 hour). Supernatants containing 'soluble' protein (containing soluble cytosolic proteins and any residual fragments of unpelleted membranes) were separated, aliquoted, rapidly frozen in and stored in liquid nitrogen. Pellets with 'membrane-enriched' protein (containing plasma, endoplasmic reticulum, mitochondria, Golgi, lysosome and peroxisome membrane proteins) were suspended in PBS containing protease inhibitor cocktail (Roche Diagnostics, Castle Hill, Australia) with 0.1% Triton X-100. Samples were aliquoted, rapidly frozen in liquid nitrogen and stored at -80°C. Protein concentration of the samples was determined using a Bradford protein assay kit (Bio-Rad, Australia).

Aliquoted protein extracts (5, 10 or 20 µg protein) were dissolved in lithium dodecyl sulfate (LDS) sample buffer (0.5% LDS, 62.5 mM Tris-HCl, 2.5% glycerol, 0.125 mM EDTA), pH 8.5, 10 minutes at 70°C. The samples were separated by electrophoresis in 4-12% bis-Tris polyacrylamide gels (Invitrogen, Australia) using MOPS-SDS running buffer and electroblotted onto PVDF membranes overnight at 4°C, according to manufacturer's recommendations (Invitrogen). Following protein transfer, blots were thoroughly washed, blocked and probed with TRPC3 antibody (batches AN-02, 03, 06 or 07; Supplementary material online, *Table S1*), and specific binding visualized using alkaline phosphatase-conjugated secondary antibody and chemiluminescence according to the manufacturer's instructions (Invitrogen). Band sizes were estimated by comparison of migration distance with Magic Mark XP protein standards (Invitrogen). The intensity of the bands corresponding to TRPC3 protein expression were determined using Photoshop CS3 (Adobe, CA, USA), normalised with corresponding actin bands and statistically analysed (GraphPad Prism, CA, USA).

To verify potential endothelial or smooth muscle cell TRPC3 expression, samples were prepared for Western blotting using rat mesenteric artery from which the endothelium had been disrupted. In freshly dissected intact vessel segments, successive and vigorous passing of a 50 μm diameter wire through the lumen disrupted the endothelium, with subsequent flushing of the lumen with Krebs solution via a micropipette to remove cellular debris. A small segment of endothelium-damaged artery was processed for confocal immunohistochemistry as described below, and compared with intact vessels for the presence of the specific endothelial marker, vWF, as confirmation of endothelial disruption.

To clarify specificity, TRPC3 antibody was incubated with its cognate peptide in order to block specific binding. Prior to use, peptide was added to antibody in a 1:10 ratio (v/v), mixed and incubated at 37°C for 1 hour, then overnight at 4°C. The blocked antibody was then used in Western blotting detection as above.

2.4 Cell culture

HEK-293 cells (Invitrogen), were cultured to 90% confluence in DMEM (Invitrogen, Australia) supplemented with 10% fetal bovine serum in a humidified atmosphere of 95% O₂/5% CO₂ at 37°C. Cells were transfected with mouse TRPC3 cDNA cloned into a pIRES-DsRed2 vector construct (Clontech, CA, USA) using Lipofectamine, 2000 (Invitrogen, Australia), according to manufacturer's instructions. Cells were treated with 1100 $\mu\text{g}/\text{ml}$ of G418 antibiotic (Invitrogen, Australia) for 4 weeks to select for stably transfected cells. The expression of mouse TRPC3 gene in the G418 resistant cells was verified by PCR amplification and sequencing of the TRPC3 cDNA transcript (primer characteristics; Supplementary material online, *Table S2*).

The sequencing of TRPC3 cDNA was made by PCR amplification of the cDNA using the BigDye Terminator V3.1 sequencing reaction mix according to the manufacturer's protocol

(Applied Biosystems, USA). The reaction product was then analyzed using ABI 3730 Capillary Sequencer (Applied Biosystems, USA) to obtain the sequence information. The TRPC3 cDNA sequence was verified via comparison with the mouse TRPC3 mRNA sequence in the NCBI database (accession no. NM_019510.2).

2.5 Mouse aortic endothelial cell calcium imaging

Aortic endothelial cells were obtained from mouse aorta explants grown on BD Matrigel™ Basement Membrane Matrix (BD Biosciences, CA, USA) as described by Suh *et al.*³ Briefly, 35 mm culture dishes were coated with BD Matrigel, diluted 1:1 with DMEM containing glucose and L-glutamine (Gibco, CA, USA) for 1-2 hour at room temperature. The excised aorta was carefully cleaned of blood and extraneous tissue, washed in PBS, cut into 2 mm rings and transferred to Matrigel-coated dishes, containing DMEM supplemented with 10% FBS (Gibco), 100 µg/ml Endothelial Cell Growth Supplement (BD Biosciences), 10 U/ml heparin (Sigma, MO, USA), 100 U/ml penicillin/streptomycin (Invitrogen, CA, USA) and 2% Minimal Essential Amino Acid mixture (Sigma). Aortic rings were cut open, placed intima-down on the gel surface and allowed to grow for 4-12 weeks to allow endothelial cells to proliferate and spread throughout the Matrigel. For calcium imaging experiments, endothelial cells were harvested from Matrigel culture following 1 hour incubation with neutral protease (7 mg/ml) in PBS, after which the cells were washed twice with cell culture medium, resuspended and plated onto 12 mm glass coverslips coated with fibronectin (BD Biosciences) and used between day 3 and 10 after the passage.

At the time of experimentation, cells were loaded with Fura-2AM (TefLabs, TX, USA) for 1 hour at 1 µg/ml and imaged by acquiring 340/380 nm fluorescent ratios every 4 seconds, using an Olympus IX81 fluorescent microscope equipped with Uplan S-Apo 20x 0.75 NA lens

(Olympus, USA), Lambda LS Xenon Arc lamp, Lambda 10-2 filter wheel shutter controller (both from Sutter Instruments, CA, USA), RET-EXi-F-M-12-C CCD-camera (QImaging, Canada) and controlled with Slidebook 4.2 Imaging software (Olympus). Experiments were performed at room temperature and continuous bath perfusion using an RC-25 bath (Warner Instruments, CT, USA). Extracellular bath solution contained (in mM): 140 NaCl, 5.6 KCl, 1.6 CaCl₂, 1 MgCl₂, 10 glucose, 10 HEPES, pH 7.3. Endothelial calcium responses to the muscarinic agonist CCh (100 μM) were measured for vehicle control (0.1% DMSO) and in the presence of Pyr3² for WT and KO derived cells. DMSO or Pyr3 was administered 5 minutes prior to commencing the calcium recording. Background fluorescence was determined from a region without cells, and was subtracted prior to ratio determination.

2.6 Immunohistochemistry

2.6.1 Fluorescence microscopy. HEK-293 cells expressing TRPC3 were fixed in 4% paraformaldehyde in PBS for 10 minutes, washed with PBS and permeabilized with 1% Triton X-100 in PBS, followed by overnight incubation with TRPC3 antibody (batch AN-03; Supplementary material online, *Table S1*) in PBS with 2.5% normal goat serum (Vector Laboratories, CA, USA). After washing, cells were incubated with AlexaFluor 488 (1:500; Invitrogen, A11008) secondary antibody in PBS for 6 hours. Following washing in PBS, cells were visualized using a Leica DMIL inverted microscope with a 40 x HCX PL Fluotar (0.75 NA) objective and I3 filter block (Leica, Mt Waverly, Australia; Ex 450-490 nm dichroic 510 Em LP 515). Images were captured using an Andor emCCD IXon camera at 1 megapixel (MP). Peptide block involved pre-incubation of primary antibody in a 1:5 (v/v) excess of the immunizing peptide (Supplementary material online, *Table S1*).

2.6.2 Confocal microscopy. The distribution of TRPC3 was examined in rat mesenteric artery, and KO and WT mouse aorta and mesenteric artery, using conventional confocal immunohistochemistry as previously described.^{4,5} The distribution of vWF was examined in arteries in which the endothelium had been disrupted compared to intact artery. Briefly, rats were perfused via the left ventricle with a clearance solution of 0.1% bovine serum albumin (BSA), 10 U/ml heparin and 0.1% NaNO₃ in saline, to fully dilate the vessels, and subsequently fixed with 2% paraformaldehyde in 0.1 mM PBS. To optimize the area visible in the narrow focal region of the IEL holes and associated potential channel localization at the IEL-smooth muscle or endothelial cell interface, as sites of potential myoendothelial microdomains,^{4,5} tubular vessel segments were cut along the lateral plane and pinned out as a flat sheet with the intima uppermost.^{4,6} In addition, some fresh vessel segments were opened, as above, and incubated for 10 minutes in Krebs' solution containing 0.1% NaNO₃, prior to fixation in 2% paraformaldehyde in PBS for 10 minutes, or acetone at 4°C for 5 minutes. Whole mount tissues were then incubated in blocking buffer, as PBS containing 1% BSA, 0.2% Triton X-100, for 2 hours at room temperature, rinsed in PBS (3 × 5 minutes) and incubated in primary antibody to TRPC3 or vWF in blocking buffer for 18 hours at 4°C (antibody characteristics, Supplementary material online, *Table S1*). Tissue was then rinsed in PBS (3 × 5 minutes) and incubated in secondary antibody (AlexaFluor 633; Invitrogen, A21070 for rat, and A21050 for mouse) diluted in 0.01% Triton X-100, for 2 hours, and further rinsed in PBS (3 × 5 minutes), mounted intima uppermost in anti-fade glycerol and examined using matched settings on a confocal microscope (FV1000; Olympus, North Ryde, Australia). Cell integrity was verified in samples of tissue via propidium iodide (0.002% in mounting media) nuclear staining. In addition to clarifying TRPC3 antibody specificity using Western blotting, transfected cells and KO mouse tissue, mesenteric artery controls involved pre-incubation of primary antibody in a 1:5 (v/v) excess of the immunizing

peptide (Supplementary material online, *Table S1*), omission of the primary, and substitution of the primary for an unrelated IgG, using the confocal labeling protocol, as above; as well as using immunoelectron microscopy data. The IEL was visualized using autofluorescence at 488 nm.

For semi-quantitative estimation of endothelial TRPC3 expression, relative pixel fluorescence density was determined using CellR software (Olympus), and a smooth muscle signal of zero, since TRPC3 are absent in these cells of this vessel.⁷ The mean fluorescence density of 10 randomly selected regions of interest, as apparent TRPC3 densities at IEL hole sites, and equivalent areas 5 μm adjacent to these areas, from each of 4 different preparations from a different animal, were determined. For comparative rat and KO mouse mesenteric artery smooth muscle fluorescence density measurements, 8 x 100 μm^2 selected regions of interest from 4 different preparations, each from a different animal, respectively, were examined.

2.6.3 Electron microscopy. Tissue preparation for immunoelectron microscopy was as previously described.^{4,8} In brief, 1-2 mm long mesenteric artery segments were rapidly dissected from heavily anaesthetized animals and frozen at high pressure (Leica bulk high pressure freezer; ~2,100 bar), freeze-substituted (Leica AFS; -90°C) in 0.1% uranyl acetate in acetone over 4 days, infiltrated, and embedded in LR gold at -25°C, and polymerized under UV light. Individual serial thin transverse sections (~100 nm) were mounted on Formvar- and carbon-coated slot grids and processed for antigen localization as for confocal immunohistochemistry, although the secondary used was 10 nm colloidal gold-conjugated antibody (1:40; 2 hours) in 0.01% Tween-20. Controls included peptide block and omission of the primary antibody. Sections were stained conventionally with lead citrate, with tissue from 3 animals being examined.

Tissue preparation and analysis for conventional serial section electron microscopy, and serial section analysis for determining myoendothelial gap junction density, was as previously

described.⁵ The IEL and the associated endothelial and smooth muscle cell regions were examined, and areas of labelling and myoendothelial gap junctions imaged at x10-40,000 on a Phillips 7100 transmission electron microscope at 16 MP (camera from Scientific Instruments and Applications, Duluth, USA).

2.7 TRPC3 and EDH-mediated vasodilation - pressure myography

The characteristics of TRPC3 channels in adult male Sprague Dawley rat mesenteric artery were determined using pressure myography. Freshly dissected rat (internal diameter in 0 mM calcium, $287 \pm 6 \mu\text{m}$; $n=15$) and mouse mesenteric arteries (internal diameter in 0 mM calcium, control, $175 \pm 8 \mu\text{m}$; $n=4$; TRPC3 KO, $167 \pm 8 \mu\text{m}$; $n=6$) were cannulated in a pressure myograph (Living Systems, Vermont, USA) and continuously superfused with Krebs' solution (37°C) at a rate of 3 ml/minute. Arteries were pressurized to 80 mmHg with incremental increases over 80 minutes. Vessels were initially pre-constricted with superfused PE (1 μM ; to 80% of maximum constriction), which was present in all experiments. Endothelium-dependent vasodilation in rat mesenteric arteries was evoked with increasing concentrations of ACh (1 nM-30 μM) added cumulatively to the bath; whilst the response in mouse mesenteric artery was evoked using the PAR-2 agonist, SLIGRL at 10 μM .⁹

Experiments were conducted in the presence of L-NAME (100 μM), ODQ (10 μM), and indomethacin (10 μM), as well as the putative TRPC3 blocker, Pyr3 (1 μM for 20 minutes²) apamin (15 minutes; 100 nM), and / or TRAM-34 (30 minutes; 1 μM), ; the latter two agents as defining blockers of EDH.¹⁰⁻¹², prior to addition of ACh or SLIGRL. Additional experiments on rat mesenteric artery were also performed in the absence of L-NAME, ODQ and indomethacin. Artery diameter changes are expressed as a percentage of the maximal dilation achieved by

replacing the control Krebs' solution with calcium-free Krebs' solution at the end of the experiment.

2.8 TRPC3 and EDH - sharp electrode electrophysiology

The characteristics of TRPC3 channels in adult male Sprague Dawley rat mesenteric artery were also determined using endothelial cell membrane potential recordings. Freshly dissected rat mesenteric arteries were cut along the longitudinal axis and pinned endothelium uppermost to the base of a recording chamber and continuously superfused as described previously.⁵ L-NAME (200 μ M) and indomethacin (1 μ M) were present in all experiments. The membrane potential of endothelial cells was recorded using intracellular glass microelectrodes containing 1 M KCl (100-140 M Ω resistance and an Axoclamp 2B amplifier: Axon Instruments, USA) and the tips were filled with Lucifer Yellow CH to allow unequivocal identification of every impaled cell.⁵ Endothelial cells were stimulated with 1 μ M ACh for 1 minute. Responses were recorded in the absence (control) and presence of Pyr3 (1 μ M), TRAM 34 (5 μ M) and apamin (100 nM). Responses recorded in the presence of blockers were expressed as a percent of the control response in L-NAME and indomethacin.

2.9 TRPC3 currents - patch clamp electrophysiology

For voltage clamp recordings, HEK-293 cells stably expressing recombinant TRPC3 channels were grown to 85-95% confluence on a coverslip coated with poly-D-lysine and collagen (Type IV from human placenta). Prior to recording, the cells were incubated in the bath solution, as HEPES-buffered physiological salt solution, containing (in mM): NaCl, 120; KCl, 5.4; MgCl₂, 1.13; glucose, 10; HEPES, 20, pH 7.3 (adjusted with NaOH) for 10 minutes, with the treatment group containing Pyr3 in the bath solution. Recording pipettes were made from borosilicate glass

(GC120TF-10, Harvard Apparatus, UK). The pipette resistance was at 3-6 M Ω and filled with internal solution containing (in mM): CsCl, 130; MgCl₂, 2.0; EGTA, 10; ATP, 0.3; GTP, 0.03; pH at 7.3 (adjusted with CsOH). Whole cell patch clamp recordings were made using an Axopatch 200 or Multiclamp 700B patch clamp amplifiers (Molecular Devices, CA, USA) controlled by pClamp v.10.2 software (Molecular Devices). The membrane was clamped at a holding voltage of -40 mV, and a voltage ramp (-100 to +50 mV) over 1 second was applied every 5 seconds.

Freshly dispersed mesenteric endothelial cells used in electrophysiological experiments were obtained from Cx40^{BAC}-GCaMP2 mice¹³ by enzymatic dissociation (70 minutes at 37°C) using neutral protease (8 U/ml) and elastase (2 U/ml) mg/ml in the following digestion buffer (in mM): 138 NaCl, 5 KCl, 1.5 MgCl₂, 0.42 Na₂HPO₄, 0.44 NaH₂PO₄, 0.1 CaCl₂, 10 HEPES, 4.2 NaHCO₃ and 0.3% BSA. These cells were used as when isolated they are easily identifiable via fluorescence microscopy. This was followed by a 1 minute incubation with collagenase type 1 (120 U/ml) in the same digestion buffer. All enzymes were obtained from Worthington (Lakewood, NJ, USA). Dispersed endothelial cells were placed in the recording chamber and identified by green fluorescence (GFP emission filter) using same microscope set up as described under Ca²⁺ imaging section. Whole cell currents of EC were recorded in the voltage clamp mode using the perforated patch configuration.¹⁴ The series resistance was maintained at or below 20 MOhm and was not compensated. The pipette solution contained (in mM) 40 KCl, 100 K gluconate, 1 MgCl₂, 10 NaCl, 0.1 EGTA, 10 NaCl, 10 HEPES, 0.1 EGTA (pH 7.2, adjusted with KOH). Extracellular bath solution (in mM): 140 NaCl, 5.6 KCl, 1.6 CaCl₂, 1 MgCl₂, 10 glucose, 10 HEPES, pH 7.3. Endothelial cells were held at -70 mV and whole cell currents were evoked by 1 second voltage ramps from -120 to +60 mV every 3 seconds. All experiments were done at

room temperature. Of note, potassium currents activated by ATP or NS 309 were analyzed after subtraction of baseline current, recorded before the agonist application.

2.10 Statistics

Agonist concentrations causing half-maximal responses (EC_{50} value) were calculated using non-linear regression analysis (GraphPad Prism) and expressed as the negative logarithm of the molar concentration (pEC_{50} values). Percentage vasodilation evoked by [agonist] was taken as the maximum (peak) responses (E_{max}). All data are expressed as mean \pm SEM from ' n ' experiments each from a different animal, and were determined by one-way analysis of variance followed by Dunnett's post-test for multiple comparisons, or paired t tests for groups of two. Calcium imaging recordings from individual cells were averaged for each coverslip (12-59 cells/coverslip). The number of coverslips for each group was from 5 to 18 from a total of 3 WT and 3 TRPC3 KO mice. The average calcium responses per coverslip were then evaluated by two-way RM-ANOVA using the Holm-Sidak test for pair-wise multiple comparison procedures. A $P < 0.05$ was considered significant.

2.11 Drugs and reagents

Electron microscopy reagents were from ProSciTech (Thuringowa, Australia), and unless otherwise stated, all other chemicals and drugs were from Sigma (Castle Hill, Australia or Saint Louis, USA), including Pyr3, or Tocris (Bristol, UK). Antibody source and characteristics are detailed in Supplementary material online, *Table S1*.

3. Results and Discussion

3.1 Rat mesenteric artery TRPC3

3.1.1 Protein localization

As a control for adequate rinsing steps in the confocal microscopy protocol, IgG alone was substituted for the primary at a matching concentration to the TRPC3 antibody in the primary antibody incubation step. Of note, when IgG alone (Supplementary material online, *Table S1*) was substituted for primary antibody, and the post-primary confocal protocol rinsing steps omitted, localized high level fluorescence densities at all internal elastic lamina (IEL) holes were present in rat mesenteric artery (data not shown); suggesting that IEL holes have an affinity for IgG; and emphasizing the importance of conducting adequate rinsing steps and control peptide block in the confocal immunohistochemistry protocol when examining whole mount vessel preparations.

3.2 Reagent characterization

3.2.1 TRPC3 antibody characterization

Specificity of the commercial Alomone TRPC3 antibody (ACC-016; Supplementary material online, *Table S1*) was demonstrated by immunohistochemistry using HEK cells expressing TRPC3 (Supplementary material online, *Figure S1A-C*) and segments of mesenteric arteries and aorta from TRPC3 KO and WT mouse (Supplementary material online, *Figures S1, S2A*, respectively), and also by Western blotting using tissue extracts of rat and mouse liver (Supplementary material online, *Figure S3*), and including primary antibody peptide block.

Four different batches of TRPC3 antibody were examined, with batches AN-02, 03 and 07 displaying consistent characteristics, whilst AN-06 did not, and was not used in subsequent work (Supplementary material online, *Table S1*). In fresh rat liver tissue extracts, TRPC3 antibody (batch AN-02) recognized an apparent monoglycosylated band at ~120 kDa, which is similar to published data for TRPC3 protein expressed in rat tissues,¹⁵ as well as a likely TRPC3 complex

at $>\sim 220$ kDa¹⁶ and a likely breakdown product at ~ 60 kDa (Supplementary material online, *Figure S3*). Degradation products of TRPC3 in tissue extracts have been noted by Clarson *et al.*¹⁵ Peptide block of the primary antibody abolished the staining of these bands (Supplementary material online, *Figure S3*) and non-specific bands remained unaffected. TRPC3 antibody batches AN-03 and AN-07 showed the same Western blot characteristics as AN-02, recognizing the same bands in the same fresh rat liver extracts (data not shown).

In rat mesenteric artery extracts, TRPC3 antibody recognized the same TRPC3 bands that were present in rat liver extracts, and also bands at ~ 110 , 80, 40 and 20 kDa (Supplementary material online, *Figure S3*), which were abolished by peptide block and which we believe represent tissue-related differences in TRPC3 breakdown products. Every care was taken to minimize protein degradation during the removal and storage of tissues. However, in some time consuming procedures, such as the dissection of fine vessels and removal of extraneous tissues, some degradation is inevitable and has affected the strength of the remaining un-degraded TRPC3 signal, particularly in the case of the vascular endothelium which forms a small relative proportional mass of the total vessel wall.

3.2.1 Pyr3 / TRPC3 blocker characterization

3.2.1.1 Pressure myography

In pressurized WT and TRPC3 KO mouse mesenteric arteries, in the presence of L-NAME, ODQ and indomethacin, SLIGRL (PAR-2 agonist; 10 μ M)-induced vasodilation was significantly attenuated in WT, but not KO in the presence of Pyr3 (1 μ M; WT, $72 \pm 7\%$ SLIGRL control, $46 \pm 9\%$ with Pyr3, $n=4$, $P<0.05$; KO $75 \pm 3\%$ SLIGRL control, 64 ± 7 with Pyr3, $n=6$, $P>0.05$).

3.2.1.2 Calcium dynamics in cultured murine aortic endothelial cells

Carbachol (CCh; 100 μ M) elicited a prolonged increase in $[Ca^{2+}]_i$ in WT and KO mouse aorta-derived primary culture endothelial cells (Supplementary material online, *Figure S2B*), and this calcium response was significantly attenuated by Pyr3 (10 μ M) in WT-derived cells, over KO-derived cells (area under the curve; reduced by \sim 54% in WT, and by \sim 24% in KO). The inhibition of the early portion of the response in KO EC corresponds to the initial phase of internal store release. This initial phase comprises the first \sim 60 seconds of the response. The sustained component of the response (following the first 60 seconds) corresponds to the Ca^{2+} influx phase and was quite different between groups. Evaluation of individual time points by the Holm-Sidak test during the sustained phase demonstrated a significant difference for the time period out to 219 seconds of the WT response. However, the corresponding sustained phase in the KO EC was largely unaffected by Pyr3. For comparison, at the 150 second time point, there was a \sim 53% inhibition in the WT cells compared with only \sim 4% in the KO. Thus, it appears that Pyr3 is selective for TRPC3-mediated Ca^{2+} influx.

3.2.1.3 Whole cell patch clamp of transfected HEK-293 cells

Carbachol (100 μ M) initiated a significant inward current (maximum, 266 ± 27 pA, $n=6$; Supplementary material online, *Figure S4A*) in transfected HEK cells expressing TRPC3 and clamped at -40 mV. This response was attenuated by \sim 84% and \sim 95%, in the presence of 2 and 10 μ M Pyr3, respectively (to 37 ± 10 and 13 ± 9 pA, $n=6$ and 4, respectively; Supplementary material online, *Figure S4B, C*).

3.2.1.4 Whole cell patch clamp of mouse mesenteric artery endothelial cells

ATP (100 μM) evoked an outward K^+ current (at 40 mV) consisting of an initial peak followed by a more sustained component (Supplementary material online, *Figure S5A, B*). Pyr3 (3 μM) inhibited the ATP-induced K^+ currents in endothelial cells such that only an initial transient component remained (Supplementary material online, *Figure S5C, D*). Pyr3 was without effect on the maximal increases in K^+ current density evoked by the S/IK_{Ca} agonist NS309 (Supplementary material online, *Figure S5E, F*).

References

1. Hartmann J, Dragicevic E, Adelsberger H, Henning HA, Sumser M, Abramowitz J *et al.* TRPC3 channels are required for synaptic transmission and motor coordination. *Neuron* 2008;**59**:392-398.
2. Kiyonaka S, Kato K, Nishida M, Mio K, Numaga T, Sawaguchi Y *et al.* Selective and direct inhibition of TRPC3 channels underlies biological activities of a pyrazole compound. *Proc Natl Acad Sci USA* 2009;**106**:5400-5405.
3. Suh SH, Vennekens R, Manolopoulos VG, Freichel M, Schweig U, Prenen J *et al.* Characterisation of explanted endothelial cells from mouse aorta: electrophysiology and Ca^{2+} signalling. *Pflugers Arch* 1999;**438**:612-620.
4. Sandow SL, Neylon CB, Chen MX, Garland CJ. Spatial separation of endothelial small- and intermediate-conductance calcium-activated potassium channels (K_{Ca}) and connexins: possible relationship to vasodilator function? *Journal of Anatomy* 2006;**209**:689-698.
5. Sandow SL, Tare M, Coleman HA, Hill CE, Parkington HC. Involvement of myoendothelial gap junctions in the actions of endothelium-derived hyperpolarizing factor. *Circ Res* 2002;**90**:1108-1113.

6. Sandow SL, Haddock RE, Hill CE, Chadha PE, Kerr PM, Welsh DG *et al.* What's where and why at a vascular myoendothelial microdomain signaling complex? *Clin Exp Pharmacol Physiol* 2009;**36**:67-76.
7. Hill AJ, Hinton JM, Cheng H, Gao Z, Bates DO, Hancox JC *et al.* A TRPC-like non-selective cation current activated by alpha 1-adrenoceptors in rat mesenteric artery smooth muscle cells. *Cell Calcium* 2006;**40**:29-40.
8. Haddock RE, Grayson TH, Brackenbury TD, Meaney KR, Neylon CB, Sandow SL *et al.* Endothelial coordination of cerebral vasomotion via myoendothelial gap junctions containing connexins37 and 40. *Am J Physiol* 2006;**291**:H2047-H2056.
9. Beleznai T, Takano H, Hamill C, Yarova P, Douglas G, Channon K *et al.* Enhanced K⁺-channel-mediated endothelium-dependent local and conducted dilation of small mesenteric arteries from ApoE^{-/-} mice. *Cardiovasc Res* 2011;**92**:199-208.
10. McGuire JJ, Ding H, Triggle CR. Endothelium-derived relaxing factors: a focus on endothelium-derived hyperpolarizing factor(s). *Can J Physiol Pharmacol* 2001;**79**:443-470.
11. Sandow SL, Tare M. C-type natriuretic peptide: a new endothelium-derived hyperpolarizing factor? *Trends Pharmacol Sci* 2007;**28**:61-67.
12. Busse R, Edwards G, Feletou M, Fleming I, Vanhoutte PM, Weston AH. EDHF: bringing the concepts together. *Trends Pharmacol Sci* 2002;**23**:374-380.
13. Tallini YN, Brekke JF, Shui B, Doran R, Hwang SM, Nakai J *et al.* Propagated endothelial Ca²⁺ waves and arteriolar dilation in vivo: measurements in Cx40BAC-GCaMP2 transgenic mice. *Circ Res* 2007;**101**:1300-1309.
14. Rae J, Cooper K, Gates P, Watsky M. Low access resistance perforated patch recordings using amphotericin B. *J Neurosci Methods* 1991;**37**:15-26.

15. Clarson LH, Roberts VH, Hamark B, Elliott AC, Powell T. Store-operated Ca^{2+} entry in first trimester and term human placenta. *J Physiol* 2003;**550**:515-528.
16. Goel M, Sinkins WG, Schilling WP. Selective association of TRPC channel subunits in rat brain synaptosomes. *J Biol Chem* 2002;**277**:48303-48310.
17. Birnbaumer L, Zhu X, Jiang M, Boulay G, Peyton M, Vannier B *et al.* On the molecular basis and regulation of cellular capacitative calcium entry: roles for TRP proteins. *Proc Natl Acad Sci USA* 1996;**93**:15195-15202.
18. Vannier B, Zhu X, Brown D, Birnbaumer L. The membrane topology of human transient receptor potential 3 as inferred from glycosylation-scanning mutagenesis and epitope immunocytochemistry. *J Biol Chem* 1998;**273**:8675-8679.
19. Wu LJ, Sweet TB, Clapham DE. International union of basic and clinical pharmacology. LXXVI. Current progress in the mammalian TRP ion channel family. *Pharmacol Rev* 2010;**62**:381-404.
20. Zhu X, Jiang M, Peyton M, Boulay G, Hurst R, Stefani E, Birnbaumer L. TRP, a novel mammalian gene family essential for agonist-activated capacitative Ca^{2+} entry. *Cell* 1996;**85**:661-71.
21. Neylon CB, Nurgali K, Humme B, Robbins HL, Moore S, Chen MX, Furness JB. Intermediate-conductance calcium-activated potassium channels in enteric neurones of the mouse: pharmacological, molecular and immunochemical evidence for their role in mediating the slow afterhyperpolarization. *J Neurochem* 2004;**90**:1414-42.
22. Chadha PS, Haddock RE, Howitt L, Morris MJ, Murphy TV, Grayson TH *et al.* Obesity upregulates IK_{Ca} and myoendothelial gap junctions to maintain endothelial vasodilator function. *J Pharmacol Exp Ther* 2010;**335**:284-293.

23. Sandow SL, Senadheera S, Bertrand PP, Murphy TV, Tare M. Myoendothelial contacts, gap junctions and microdomains: anatomical links to function? *Microcirculation* 2012;**19**:DOI10.1111/j.1549-8719.2011.00146.x.
24. Dora KA, Gallagher NT, McNeish A, Garland CJ. Modulation of endothelial cell $K_{Ca}3.1$ channels during endothelium-derived hyperpolarizing factor signaling in mesenteric resistance arteries. *Circ Res* 2008;**102**:1247-55.

Table S1. Primary antibody characteristics.

Antibody (anti)	Raised against species / antigen	Antigen peptide block	Working dilution	Supplier, catalog and batch / lot number/s	Host
TRPC3*	Mse C' aa 822-835	yes	8 µg/ml, IHC / IEM 0.8 µg/ml HEK cell IHC 0.8 µg/ml Westerns	Alomone, ACC-016; batches AN-02,03,06 [#] ,07	rabbit
vWF	Purified Hu vWF	no	1:300	Sigma, F3520	rabbit
IgG	Purified Rb IgG	no	5 µg/ml	Chemicon, PP64	rabbit

aa, amino acid; Hu, human; IEM, immunoelectron microscopy; IHC, immunohistochemistry; Mse, mouse; Rb, rabbit. *shares ~93% (13/14 residues) sequence identity with rat TRPC3. [#]AN-06 showed variability in Western blot and immunohistochemical characteristics compared to other TRPC3 antibody batches, and was thus not used in the primary aspects of this study.

Table S2. TRPC3 primer characteristics.

	Sequence (5' to 3')	Relative position from the start codon
Forward	CTAACTTTTCCAAATGCAGGAGGAGAAG	2135
Reverse	TCGCATGATAAAGGTAGGGAACACTAGA	2630

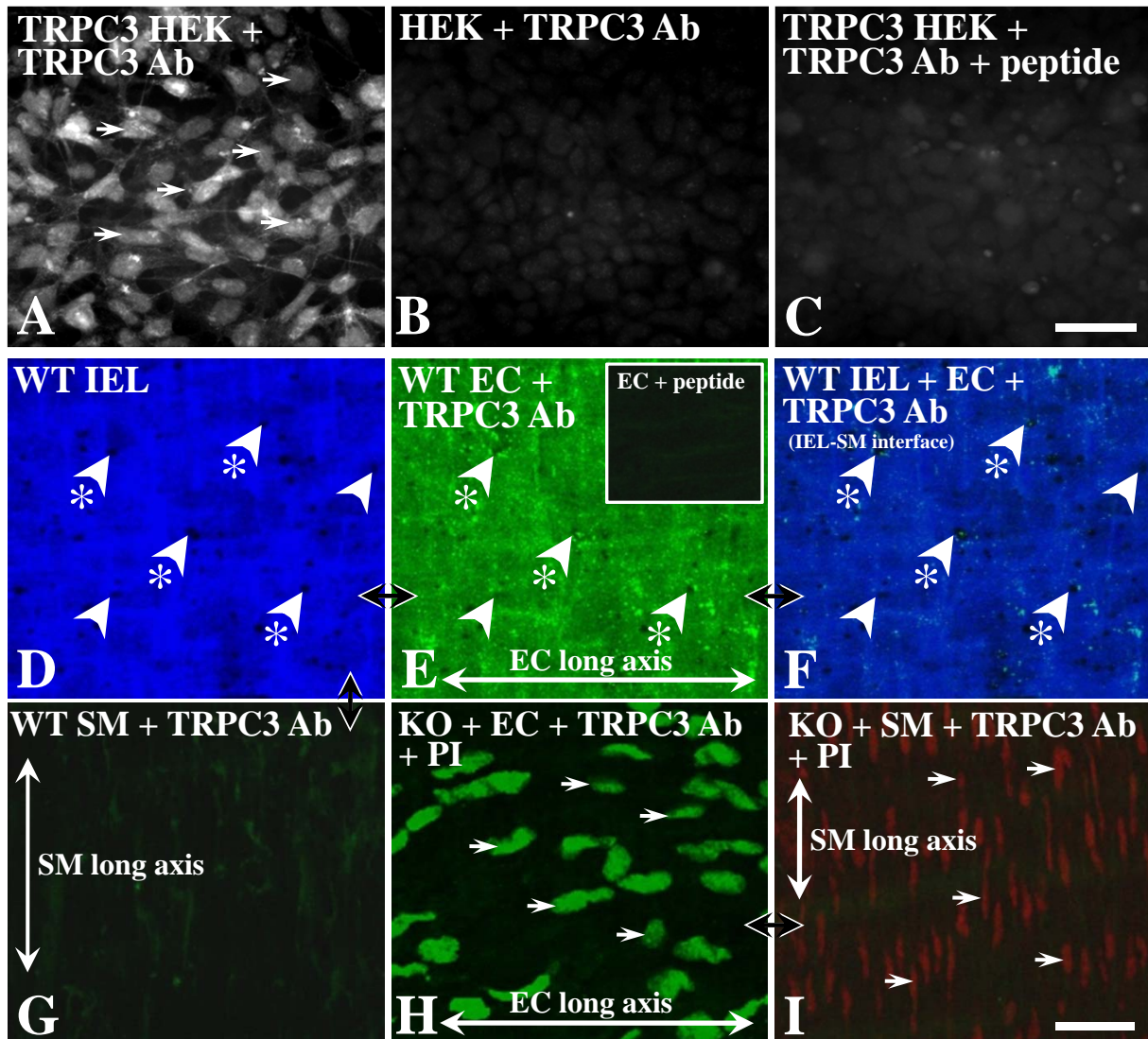


Figure S1. TRPC3 antibody characterization in transfected HEK cells and control and TRPC3 knock-out mouse mesenteric artery using immunohistochemistry. TRPC3 antibody (Ab; Alomone ACC-016; AN-03, shown as example; Supplementary material online, *Table S1*) specificity was supported via use of transfected cells expressing mouse TRPC3 cDNA. TRPC3 transfected HEK cells labelled with TRPC3 antibody (A; examples with arrows), whilst incubation of untransfected cells (B) and peptide block (C) show an absence of labelling, as did primary antibody omission, under the same conditions as A (data not shown). Consistent labelling was found using TRPC3 Ab batches AN-02, 03 and 07, whilst 06 showed an absence of labelling, and was not used in subsequent protocols. In mesenteric artery from control wild-type (WT) and TRPC3 knock-out (KO) mice (D-G and H, I, respectively), TRPC3 antibody (AN-07; Supplementary material online, *Table S1*) specificity was further characterized. TRPC3 confocal immunohistochemistry demonstrated the presence of TRPC3 in endothelial cells (EC), but not the smooth muscle (SM) of WT mesenteric artery (E, F, respectively). Similar to rat mesenteric artery (*Figure 1*), discrete holes are present in the internal elastic lamina (IEL) between the endothelium and smooth muscle (dark spots; D, F). Low level diffuse TRPC3 is localized to the endothelial membrane (E), whilst overlay of IEL and TRPC3 label at the IEL-SM focal plane border shows strong TRPC3 expression at a proportion of IEL holes (F; examples, arrowed with asterisks), as potential myoendothelial microdomain sites; noting that not all such sites have localized TRPC3 densities (examples with arrows, D, F). TRPC3 was absent in both cell layers of vessels from TRPC3 KO mouse (H, I). Peptide block abolished staining in WT mesenteric artery (E, inset), whilst cell layer patency was verified with propidium iodide (PI) nuclear staining (arrows, H, I, for example). The same vessel region is shown for WT and KO panels (D-G and H, I, respectively); with longitudinal vessel axis left to right. Internal elastic lamina (IEL) autofluorescence assisted with differentiation of cell layers (eg. D). $n=3-4$, each from a different animal. NB. H, I panels have been contrast/brightness enhanced in Photoshop. Scale bar, 50 μm (A-C), 25 μm (D-I).

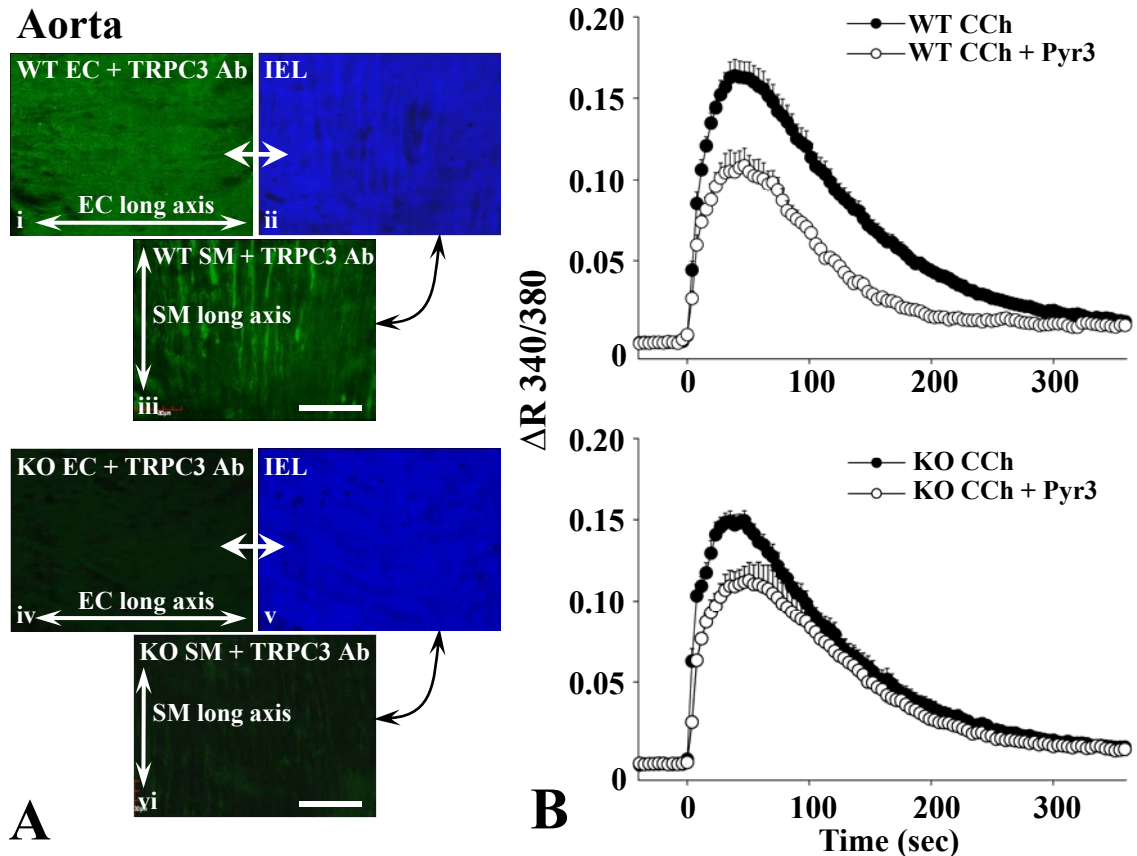


Figure S2. Mouse aorta TRPC3 distribution and agonist-induced calcium effects of Pyr3-block in isolated aortic endothelium. Antibody (Ab) specificity was further tested using TRPC3 knock-out (KO) and control wild-type (WT) tissue (A, B), with mouse genotypes being confirmed by PCR amplification of genomic DNA. TRPC3 antibody (AN-07; Supplementary material online, *Table S1*) confocal immunohistochemistry demonstrated the presence of TRPC3 in aortic endothelium (EC) and smooth muscle (SM; A). TRPC3 was absent in both cell layers of vessels from TRPC3 KO mouse (A, iv, vi). Peptide block abolished staining in WT aorta, whilst cell layer patency was verified with propidium iodide (PI) nuclear staining (see Supplementary material online, *Figure S2*, for example). The same vessel region is shown for WT and KO panels (A, i-iii and iv-vi, respectively); with longitudinal vessel axis left to right. Internal elastic lamina (IEL) staining assisted with differentiation of cell layers (A, ii, v). $n=3-4$, each from a different animal. Scale bar, 40 μm . TRPC3 blocker efficacy was tested using primary cultured aortic ECs derived from TRPC3 KO and WT mice. The putative TRPC3 blocker Pyr3 caused significantly larger attenuation of the sustained carbachol (CCh; 100 μM)-induced calcium response in control WT (B, upper), compared to TRPC3 KO (B, lower) ECs. Cells were preincubated with Pyr3 (10 μM) or 0.1% DMSO (control) for 5 minutes before recording. Calcium data represent the mean responses per coverslip \pm SEM, obtained from three WT and three TRPC3 KO mice ($n=3$ different animals each, for WT and KO). The number of coverslips per group (n) were control WT, 18; WT + Pyr3, 5; KO control, 10; and KO + Pyr3, 5.

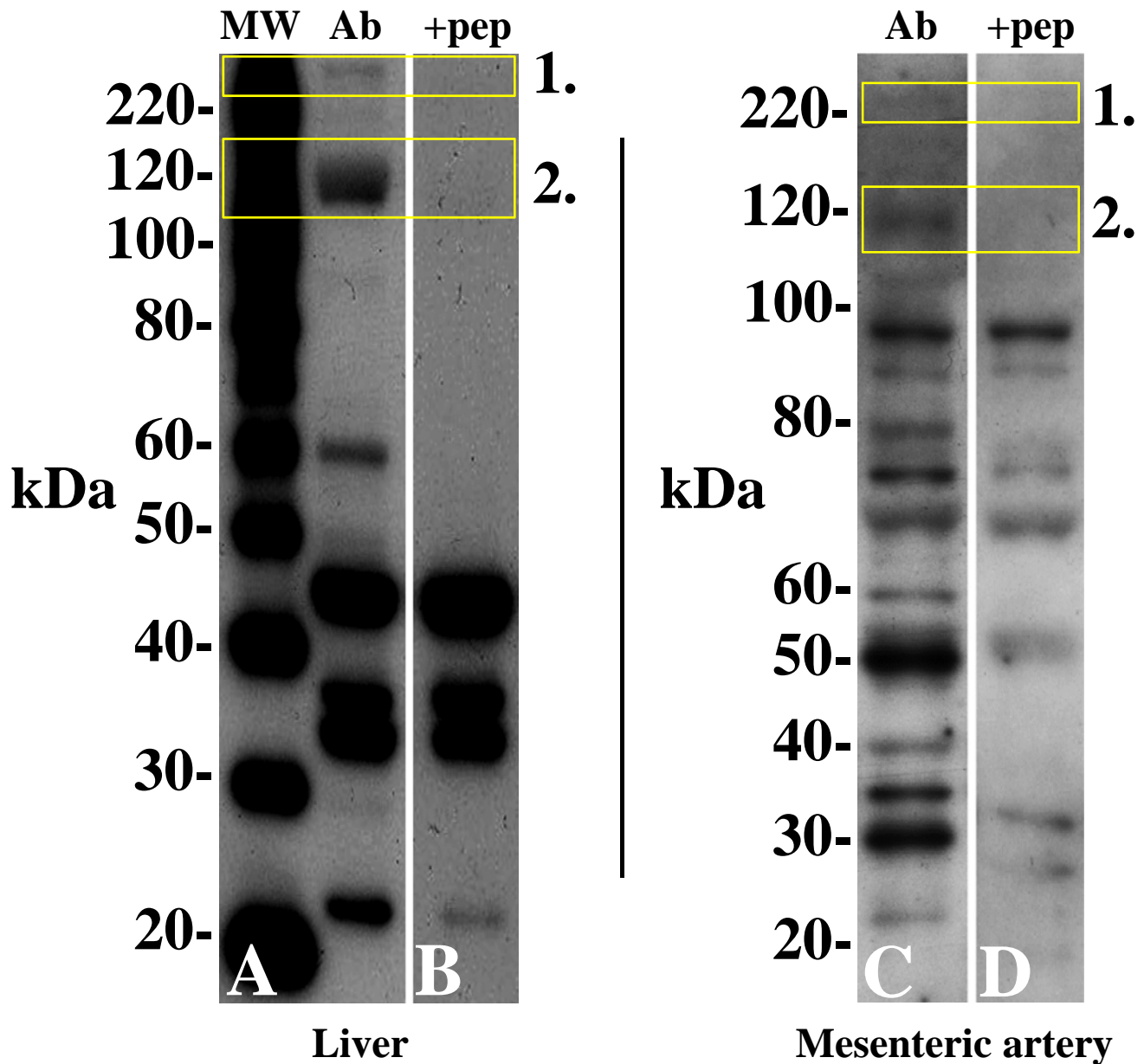


Figure S3. Western blot of TRPC3 protein expression in rat liver and mesenteric artery, with peptide block. Antibody (Ab) specificity was examined using control rat liver (A, B) and mesenteric artery (C, D) with peptide block. TRPC3 antibody batches AN-02 (as example used here), 03 and 07 (Supplementary material online, *Table S1*) were characterized using Western blotting. AN-02, 03 and 07 recognize monoglycosylated TRPC3 protein as a band at ~120 kDa (A2, boxed), whilst the band at >~220 kDa (A1, boxed) is probably an aggregate / undissociated TRPC3 channel complex, as a slow migrating band; whilst the ~60 kDa band is a likely breakdown product of the TRPC3 protein. Peptide block (+ pep) removed the TRPC3 bands (B, D, boxed, 1, 2). For liver, four lanes in total were run (two representative shown), with tissues from one rat per lane and loading of 5 μ g of protein; whilst for the mesenteric artery three lanes in total were run with tissue from four different rats pooled together with loading of 10 μ g of protein per lane. Incubation with a 1:10 (v/v), excess of peptide removed the TRPC3 bands (B, D, boxed, 1, 2). MW, molecular weight.

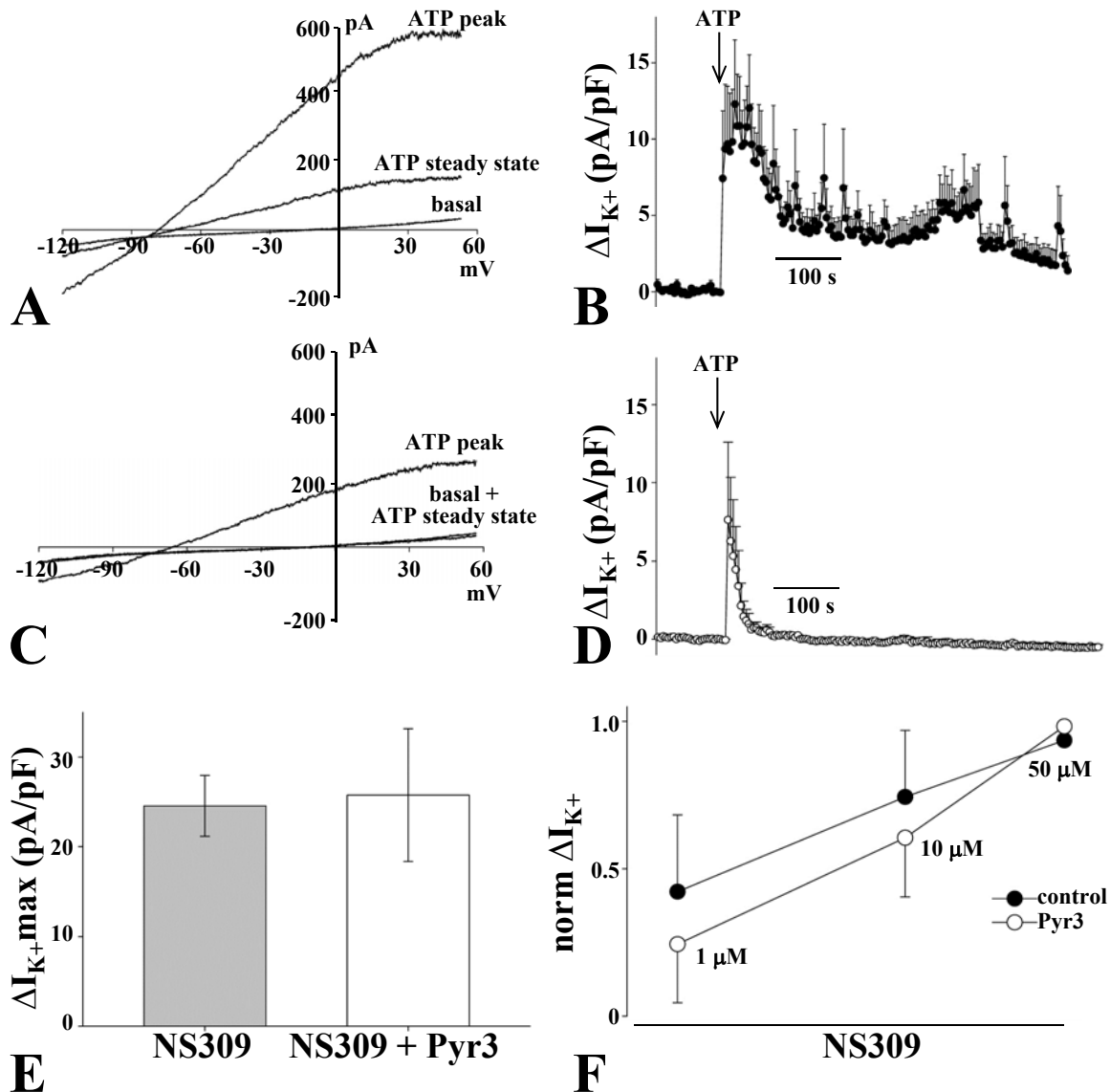


Figure S4. Pyr3 effect on agonist-induced K^+ currents in mouse mesenteric artery endothelial cells using patch clamp. ATP activates IK_{Ca}/SK_{Ca} -like potassium current in mesenteric artery endothelial cells (A, B). Representative I-V traces (A), and time-dependent changes in ATP (100 μ M)-activated potassium current density; $n=8$ cells, from five mice (B). TRPC3 channel blocker Pyr3 (3 μ M) inhibits ATP-activated potassium current (C, D; same protocol as A, B, respectively, but with addition of Pyr3). Representative I-V traces (C), and time-dependent changes in ATP-activated potassium current density in cells pretreated with Pyr3 (2-5 minutes before the ATP; $n=4$ cells, from four mice; D). Pyr3 (added 2-5 minutes before the NS309; $n=5$), had no effect on maximal potassium current density induced by the S/IK_{Ca} agonist NS309 alone (50 μ M; $n=4$; E). Concentration-response plot (normalized to maximum) for potassium current density from a subset of cells exposed to NS309, with or without Pyr3 pretreatment ($n=3$ in each group; F). B, D were recorded at +40 mV. Mean \pm SEM.

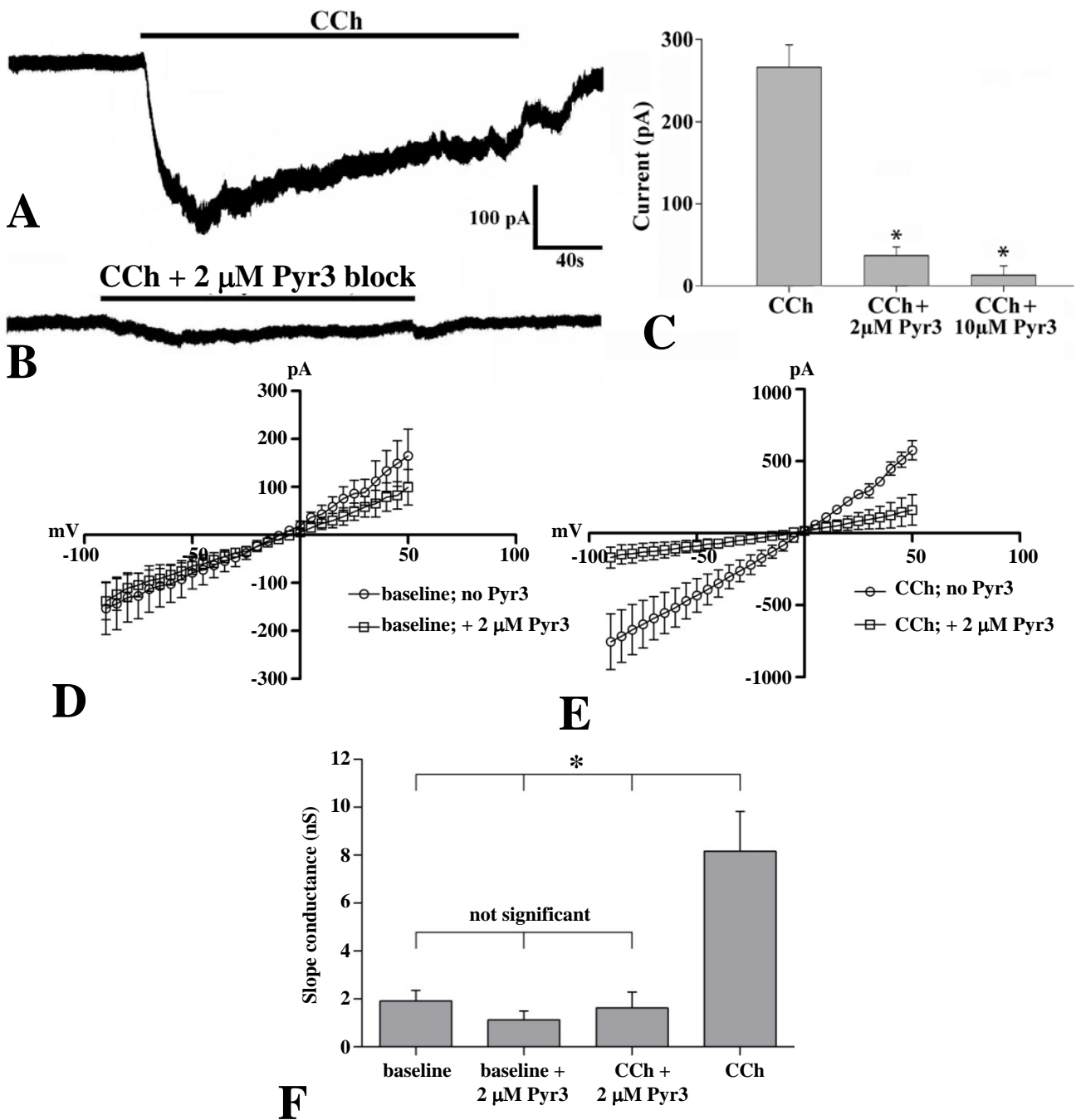
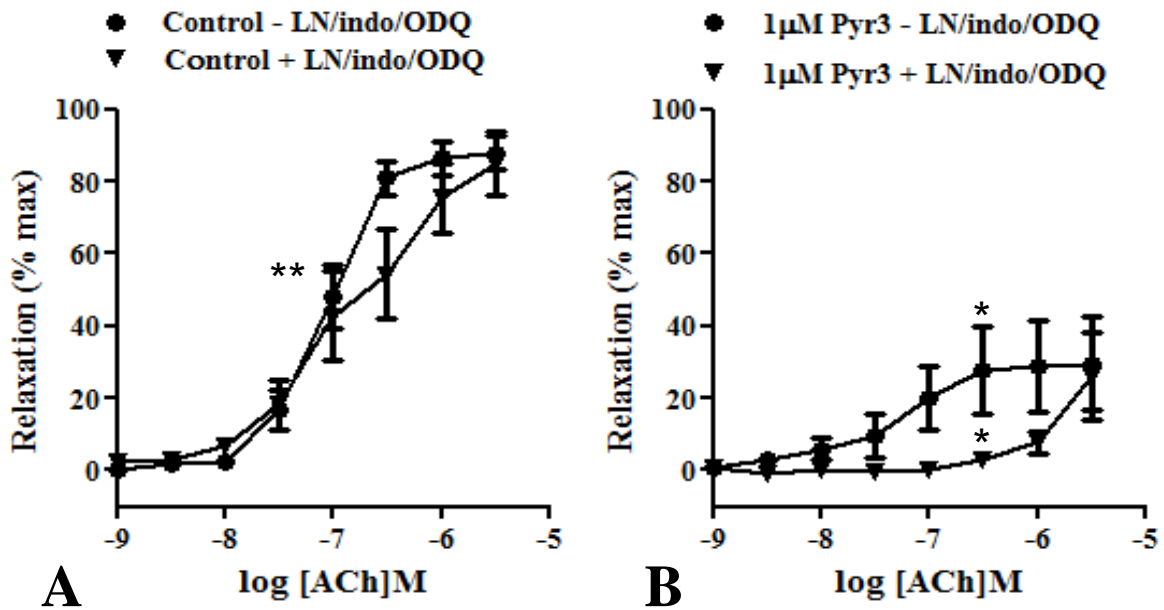


Figure S5. Characterization of specificity of Pyr3 block of TRPC3 channel conductance in HEK-293 cells.

The potency of the putative TRPC3 channel blocker Pyr3 was tested using patch clamped HEK cells transfected with TRPC3 plasmid. Carbachol (CCh; 100 μ M)-activated an inward TRPC3 current (example, A) that was significantly attenuated by Pyr3 at 2 and 10 μ M (B, C; $n=6$ and 4, respectively, vs $n=6$ for control CCh response). Current / voltage (I/V) relationships of baseline currents (D) show that Pyr3 has no significant effect on the intrinsic I/V profile; whilst I/V plots show Pyr3 block of CCh-activated inward and outward TRPC3 current (E). I/V plots were derived from voltage ramps over 1 sec; with data from an average of 3 cells per trace. Histogram of slope conductances (F, measured between -60 and -20 mV) for HEK293 cells expressing TRPC3 shows Pyr3 inhibition that returns CCh-activated TRPC3 conductance to baseline (F; $n=5$, for each group). Mean \pm SEM. * $P<0.05$, significant.



C	pEC ₅₀	E _{max}	n
1. Vehicle (ACh)	7.0 ± 0.1**	87.9 ± 2.8	7
2. Vehicle + L-NAME / ODQ, indomethacin	6.4 ± 0.1**	94.3 ± 2.1	14
3. Vehicle + Pyr3 (1 µM)	7.1 ± 0.2	29.9 ± 5.7 [#]	7
4. Vehicle + L-NAME / ODQ, indomethacin + Pyr3	-	26.0 ± 12.1 [#]	5

Figure S6. Endothelium-dependent relaxation in rat mesenteric artery. In pressurized rat mesenteric arteries, relaxation to ACh (1 nM-100 µM) was examined in the absence (A) and presence (B) of Pyr3 (1 µM) in the absence (A, B, circles) and presence (A, B, triangles) of L-NAME (100 µM), ODQ (10 µM) and indomethacin (10 µM) to clarify the relative potential contribution of TRPC3 to EDH, and NO/prostaglandin-mediated relaxation. Each *n* is from a different animal. *P*<0.05 indicates difference in *, for 0.3 µM ACh (in B); **pEC₅₀, between controls (in A; see also C); [#]E_{max}, relative to matched ACh controls (C). Data for + L-NAME, ODQ and indomethacin are from *Figure 2* and *Table 3*.

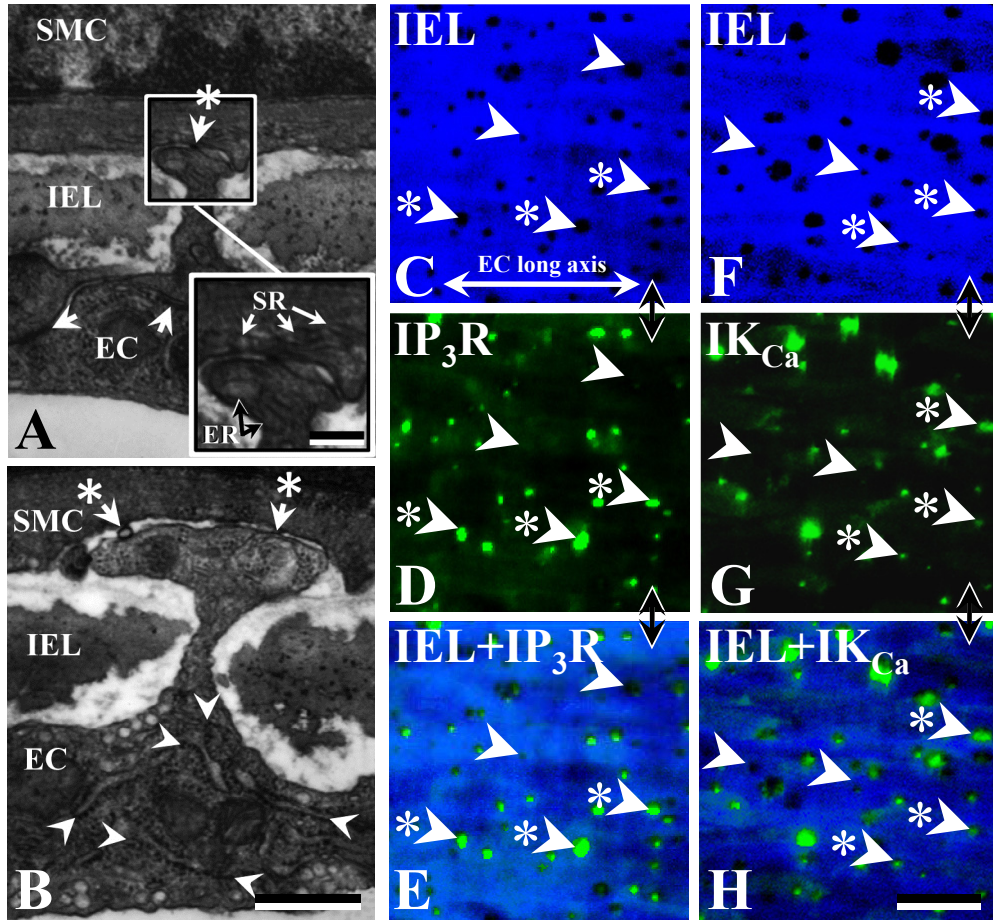


Figure S7. Ultrastructure of selected close myoendothelial contact sites and confocal immunohistochemistry of IP_3R and IK_{Ca} in rat mesenteric artery. At selected endothelial cell (EC) and smooth muscle cell (SMC) contact sites of ≤ 30 nm, smooth endoplasmic and sarcoplasmic reticulum (ER/SR; *A*) and rough ER (*B*; arrowed) are present in and near the associated EC projection (*A*, *B*). Small regions of myoendothelial gap junction membrane are also present (arrow with asterisk, *A* and inset; *B*), as are EC-EC gap junctions near such sites. Of note, in rat mesenteric artery, only a proportion of close myoendothelial contact sites have apparent accumulations of ER and / or SR. In a similar manner, inositol-1,4,5-trisphosphate receptor (IP_3R) and intermediate conductance calcium-activated potassium channel (IK_{Ca} , as IK_1) are localized to a proportion of internal elastic lamina (IEL) hole sites (dark spots), at the IEL-SM focal plane border, as potential sites of close myoendothelial contact (*C-E* and *F-H*, respectively; examples at arrowheads with asterisks; using antibodies to pan- IP_3R and IK_1 , from Chemicon (AB1622) and Craig Neylon,²¹ University of Melbourne (respectively). Lower level diffuse IP_3R and IK_{Ca} is also localized to the endothelial membrane (*D*, *G*, respectively). IEL holes without accumulations of IP_3R or IK_{Ca} are also present (*C-H*, examples at arrowheads without asterisks). Of note, IEL panels (*C*, *F*) have been contrast/brightness enhanced in Photoshop. Peptide block and incubation in secondary antibody alone resulted in no labelling (data not shown), with antibody characterization, as per previous studies.^{4,6,22} Longitudinal vessel axis left to right, with $n=3$, each from a different animal (*C-H*). Scale bars, 1 μm (*A*, *B* main), inset, 200 nm (*B*), 25 μm (*C-H*). Data from adult male rat second and third order vessels. Panels *A-E* from,²³ with permission; *F-H*, Sandow, unpublished results (see also^{4,6,24}).